JOURNAL OF GUIDANCE, CONTROL, AND DYNAMICS
Vol. 23, No. 5, September–October 2000

Experiments on Control of Limit-Cycle Oscillations in a Typical Section

Kenneth D. Frampton* and Robert L. Clark†
Duke University, Durham, North Carolina 27708

The experimental application of active control to reduce or eliminate limit-cycle oscillations in a typical section airfoil is presented. The test rig consists of a three-degree-of-freedom typical section which has free play in the flap restoring stiffness. Such a free play was intended to mimic that associated with control surface mechanism backlash in a real system. Control is effected by means of an actuator acting on the flap. A linear quadratic Gaussian optimization scheme is used to design a compensator that will accomplish three goals: 1) reduce or eliminate limit-cycle oscillations, 2) increase the flutter boundary, and 3) be robust to variations in the flow velocity. Although the typical section is a nonlinear dynamic system, the control system design was based on the linear typical section with no free play. The results presented indicate that each of these goals was accomplished. More specifically, limit-cycle oscillations were eliminated, the flutter velocity was increased by 17%, and the control system was stable over a wide range of flow conditions.

Nomenclature

J	= cost function
Q_e	= disturbance noise weight
Q_r	= performance weight
q_{flap}	= flap-sensor voltage
q_{pitch}	= pitch-sensor voltage
q_{plunge}	= plunge-sensor voltage
R_e	= sensor noise weight
R_r	= control effort weight
T_{zw}	= disturbance-to-performance system transfer function
U	= flow velocity
$\boldsymbol{u}$	= control voltage
$\boldsymbol{w}$	= disturbance input vector
$\boldsymbol{y}$	= sensor output vector: $\{q_{\text{pitch}}\ q_{\text{plunge}}\ q_{\text{flap}}\}$
$\boldsymbol{z}$	= performance vector

Introduction

A SERIES of investigations has been undertaken to investigate limit-cycle oscillations in a typical section with free play and to demonstrate the effectiveness of feedback control in improving the aeroelastic response.[1–4] Previous investigations studied the response of a three-degree-of-freedom typical section model with a control surface both analytically and experimentally.[1] This study revealed the limit-cycle behavior of the system throughout the stable flow regime. This behavior included a chaotic transition region among other interesting limit-cycle patterns.

Many other references exist for the modeling and analysis of nonlinear aeroelastic systems such as those in Refs. 5–13. Results presented by Vipperman et al.[2] served to demonstrate that the control surface can be used to provide successfully gust alleviation and extend the flutter boundary for a three-degree-of-freedom, linear, aeroelastic model. Vipperman et al.[3] also demonstrated that robust control strategies can be applied in the design of compensators for a family of dynamic pressures.

The purpose of this investigation is to experimentally implement linear quadratic Gaussian (LQG) control for the purpose of diminishing or eliminating this type of limit-cycle oscillations. The approach taken here is to design an LQG compensator based on the typical section with no free play (i.e., the control system is designed based on a linear system). This compensator is then used to close the loop around the nonlinear typical section with free play in the flap-restoring force. The typical section model, experimental setup, and control system design are described in subsequent sections. This is followed by a presentation and discussion of the results.

Received 5 February 1999; revision received 5 February 1999; presented as Paper 99-1466 at the AIAA/ASME/ASCE/AHS/ASC Structures, Structural Dynamics, and Materials Conference, St. Louis, MO, 12–15 April 1999; accepted for publication 10 September 1999.

*Research Assistant Professor, Department of Mechanical Engineering; currently Assistant Professor, Vanderbilt University, Department of Mechanical Engineering, Box 1592 Station B, Nashville, TN 37235. Member AIAA.

†Associate Professor, Department of Mechanical Engineering, Box 90300. Member AIAA.

Experimental Equipment

The experimental equipment is described in this section including the typical section model, the low-speed wind tunnel, and the signal processing test equipment.

Typical Section Model

The experimental model is shown in Fig. 1. This is the same experimental equipment employed by Vipperman et al.[2,3] and very similar to that studied by Conner et al.[1] The wing was based on a NACA-0012 airfoil shape consisting of a main wing with a 19-cm chord and 52-cm span and a trailing-edge flap with a 6.35-cm chord and 52-cm span, which rotates relative to the main wing about a pinned axis.

The pitch and flap positions were measured with rotational variable displacement transducers (RVDTs) mounted to the upper ends of the flap and wing rotational axes to measure the angular deflection of each airfoil independently. The pitch position was also measured with an RVDT mounted to ground and attached to the upper support platform for the wing. The three RVDT signals serve as the control system inputs as well as the performance variables for the control system design. A more detailed description of the typical section hardware is provided by Conner et al.[1] and by Vipperman et al.[2,3] This system had a flutter velocity of 18.8 m/s, and the resonant frequencies associated with the pitch, flap and plunge motion are 3.7, 15.0, and 7.0 Hz, respectively.

Flap Stiffness Free Play

The nonlinearity in this system resulted from free play in the flap-restoring force. Such a free play was intended to mimic that associated with control surface mechanism backlash in a real system. The flap stiffness was provided by a thin steel rod that was cantilevered off of the flap rotational shaft. The other end of the rod could be rigidly anchored to the wing base. Or, as was done in these experiments, the end of the rod could be permitted to float between two stops. When in this configuration, the flap stiffness was zero within this free-play region. When the flap stiffness rod struck one of the boundary pins, it reverted to its linear stiffness configuration. This resulted in a piecewise, nonlinear restoring force.[1]

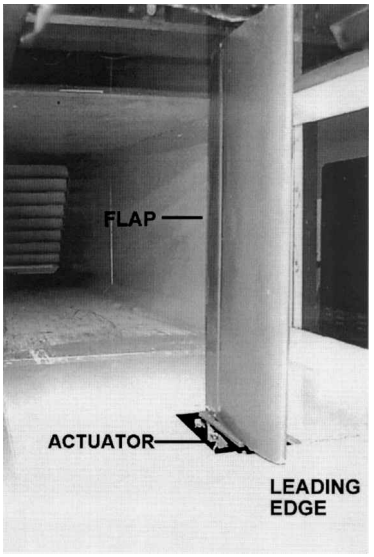

Fig. 1 Photograph of the typical section experimental model mounted in the Duke University low-speed wind tunnel.

Wind Tunnel

All tests of the two-dimensional wing model were performed in the Duke University wind tunnel. The wind tunnel is a closed-circuit tunnel with a test section of 0.70 × 0.51 m and a length of 1.22 m (see Fig. 1). The maximum attainable air speed is 89 m/s. For the present test the Reynolds number based upon model chord is 0.52×10^6.

Signal Processing

Both analog and digital signal processing equipment were used to implement the control systems and measure the performance. The control systems were discretized and implemented using a TMS320C40-based digital signal processor (DSP) board installed in a personal computer. Analog, high-pass gain amplifiers were used to increase the sensor signals in order to take full advantage of the DSP board's dynamic range.

The time trace data and frequency-domain signal analysis were performed using a four-channel Siglab spectrum analyzer. System identifications were performed for the purpose of control system design. This was accomplished by curve fitting the measured linear system transfer functions for each of the three control path transfer functions using SmartID software.[14] The system was made linear by setting the flap free play to zero. Hence, all control system designs are based on a linear model identical to the nonlinear model excepting the free play. The derived state-space models contained 18 states and agreed very well with the measured transfer functions. The states of this model were of mathematical construct and have no specific physical interpretation.

Control System Design

The block diagram of the model presented in Fig. 2 was used to synthesize the controllers for the purpose of this work. The first step toward compensator design was to obtain a system identification based on the linearized model (i.e., no flap free play). Then, an $\mathcal{H}_2$-synthesis technique was employed to design compensators at several discrete flow speeds ($U = 1, 2, 3, \ldots, 18$ m/s). In previous work[3] a single dynamic compensator was designed to operate over the entire flow regime; however, for the purpose of this study, the objective was to determine the ability of the control system to eliminate limit-cycle oscillations (LCOs) at each flow speed.

Both process noise and sensor noise were used as disturbance inputs, and the cost function was constructed from the square of the 2-norm between the error $\boldsymbol{z}$ and the disturbance $\boldsymbol{w}$ (see Fig. 2). The cost function, which was minimized, can be expressed mathematically as follows:

$$J = \lim_{t \to \infty} \left(E[\boldsymbol{z}^T(t)\boldsymbol{z}(t)] \right) = \| T_{zw} \|_2^2 \tag{1}$$

where T_{zw} is the closed-loop transfer function between $\boldsymbol{z}$ and $\boldsymbol{w}$. For the purpose of this work, the disturbance $\boldsymbol{w}$ was composed of both process noise and sensor noise as is typical of LQG design. The error

Table 1 Compensator design weights

Flow velocity, m/s	Control effort penalty, R_r	Sensor noise weight, R_e
7	0.04	0.5
8	0.10	1.0
9	0.10	2.0
10	0.10	2.0
11	0.10	2.0
12	0.10	2.0
13	0.10	2.0
14	0.10	3.0
15	0.10	3.0
16	0.10	3.0
17	0.10	3.0
18	0.10	3.0

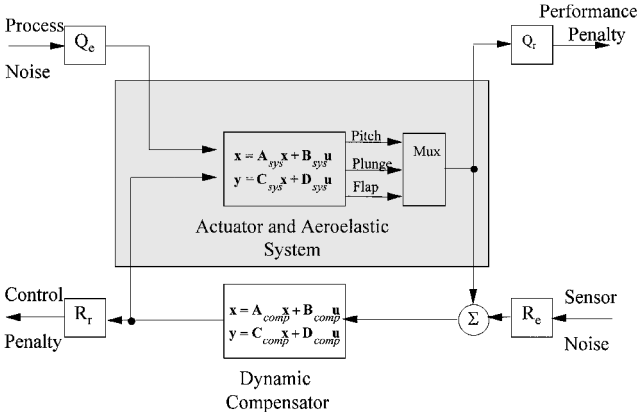

Fig. 2 Schematic of the control system design.

outputs $\boldsymbol{z}$ were constructed from a scalar weighting of the response in wing pitch, plunge, and flap position as well as a control effort as follows:

$$z = \begin{bmatrix} Q_r^{\frac{1}{2}} & 0 \\ 0 & R_r^{\frac{1}{2}} \end{bmatrix} \begin{Bmatrix} y \\ u \end{Bmatrix} \tag{2}$$

where R_r is a scalar, y is a vector containg the pitch, plunge and flap sensor voltages, and u is the control actuator input voltage. The weighting matrix Q_r is defined as

$$Q_r = \begin{bmatrix} q_{\text{pitch}} & 0 & 0 \\ 0 & q_{\text{plunge}} & 0 \\ 0 & 0 & q_{\text{flap}} \end{bmatrix} = \begin{bmatrix} 1 & 0 & 0 \\ 0 & 5 & 0 \\ 0 & 0 & 1 \end{bmatrix} \tag{3}$$

which affects the relative weighting of the pitch, flap, and plunge performance variables. Note that the input u was penalized to prevent excessive control voltages. These design parameters were fixed over all flow speeds investigated and were selected to make each performance measure scale equally. The final control effort penalty R_r and the sensor noise weights R_e are listed in Table 1. In each case the value selected was the maximum value that resulted in elimination of the limit-cycle behavior. Thus, each value represents the minimum control effort required to achieve the desired performance.

Results

Results from the experimental investigation are presented in this section. Open-loop limit-cycle data will be discussed first followed by a discussion of the application of LQG control to alleviate LCOs. Next, the ability of the control system to increase the flutter boundary will be presented along with a discussion of the robustness of the compensator to variations in system parameters.

Open-Loop Limit-Cycle Behavior

Previous investigations of the LCOs exhibited by this typical section model in a slightly different configuration were published by Conner et al.[1] The typical section model in its current configuration

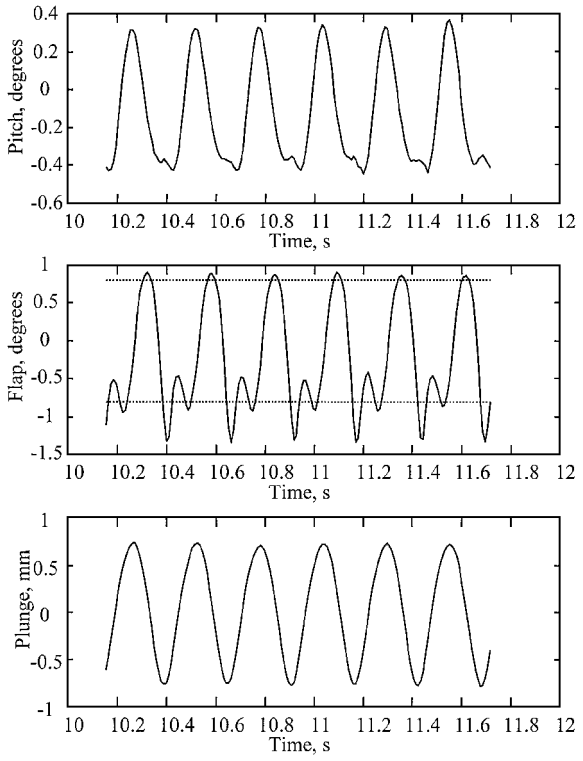

Fig. 3 Limit-cycle behavior for $U = 7$ m/s.

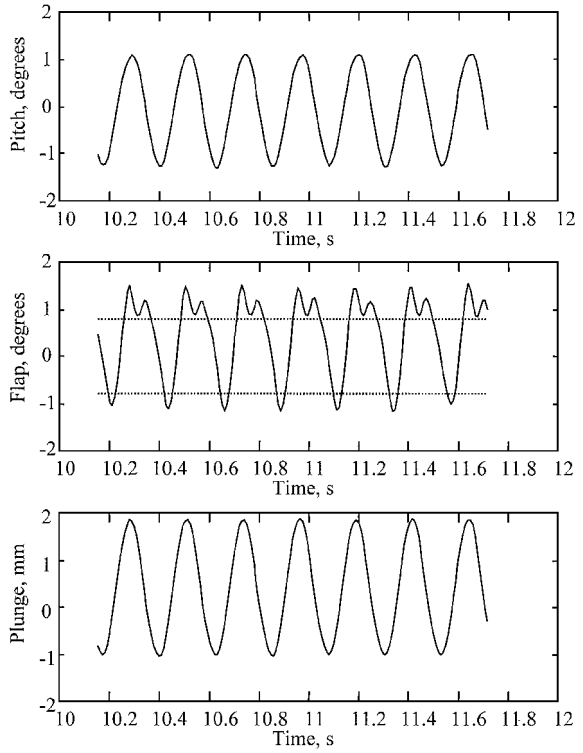

Fig. 4 Limit-cycle behavior for $U = 15$ m/s.

showed a slightly different LCO behavior. Most notably, the current configuration did not have the chaotic LCO transition region demonstrated by Conner et al.[1] Figure 3 shows several cycles of a typical limit cycle for the pitch, flap, and plunge motion when $U = 7$ m/s. Note that the flap exhibits a tap-tap motion against one side of the free-play region (limits of the free-play region are denoted by the dashed lines). This behavior was also noted by Conner et al.[1] Figure 4 depicts the limit-cycle oscillations for a flow velocity of $U = 15$ m/s. Note that the tap-tap behavior is still present; however, it has shifted to the other side of the free-play region.

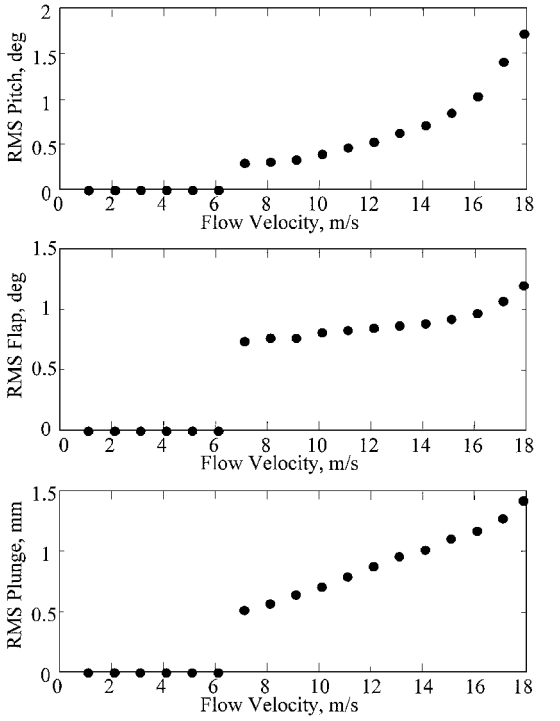

Fig. 5 RMS limit-cycle amplitude.

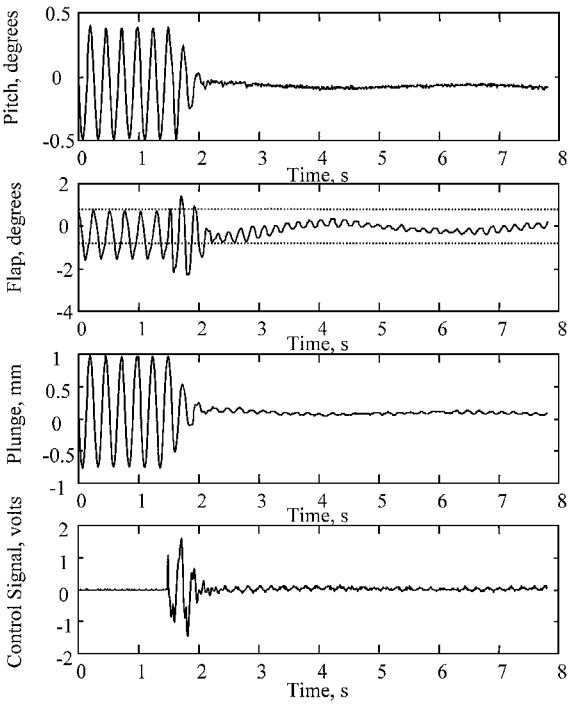

Fig. 6 Compensator performance for $U = 7$ m/s.

The rms amplitude of the LCO motion is shown for all stable flow speeds in Fig. 5. Note that the limit-cycle motion begins at a flow speed of $U = 7$ m/s, and the amplitude grows steadily until it reaches the flutter velocity of $U = 18.8$ m/s. These results are consistent with those reported by Conner et al.[1] as well as Vipperman et al.[2,3]

Limit-Cycle Alleviation with LQG Control

An LQG compensator was designed based on a linear system identification for each flow speed as already described. The effectiveness of this approach is demonstrated in Fig. 6 for a flow speed of $U = 7$ m/s. This figure shows a time history of the airfoil pitch, flap, and plunge motion in limit-cycle motion as well as the control signal. After approximately 2 s of LCO motion, the control

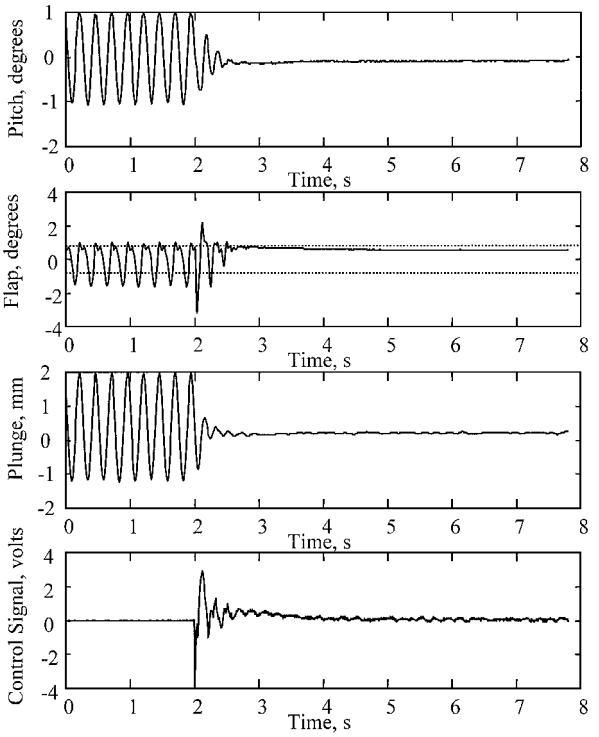

Fig. 7 Compensator performance for U = 12 m/s.

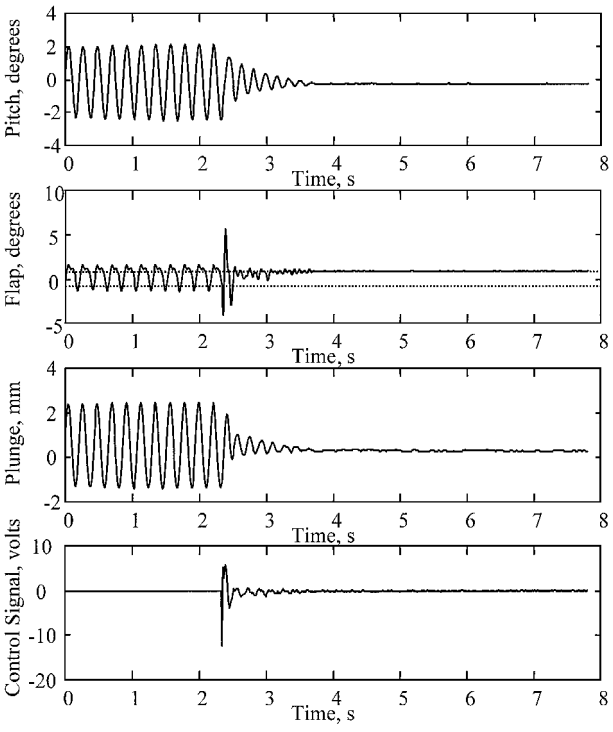

Fig. 8 Compensator performance for U = 17 m/s.

system was activated. (The exact time of control system initiation is apparent in the control voltage plot). Note that after the control system is activated the limit cycles are quickly reduced. The system settles into a dominantly low-frequency motion (clearly apparent in the flap motion plot), which gradually decays with time. The system also exhibits a low-amplitude limit cycle at the open-loop LCO frequency. This lightly damped, low-frequency motion only occurred for flow speeds below $U = 9$ m/s. Above this flow velocity the control system succeeds in eliminating the oscillatory motion of the airfoil altogether. This is demonstrated in Fig. 7, which shows the time history for $U = 12$ m/s. Again, the airfoil is moving in its limit-cycle motion, and the control system was activated after approximately 2 s. When the control system is engaged, the limit cycle quickly decays, and the airfoil settles into a nearly static equilibrium. The system is stabilized with the flap positioned inside the free-play region. This indicates the control system is providing most of the restoring force for the flap motion. It also indicates that the aerodynamic equilibrium of the flap position is inside the free-play zone. At higher flow velocities this was not the case.

The control system continued to be effective throughout the open-loop stable flow regime. Figure 8 shows the closed-loop response for $U = 17$ m/s. Once again the limit-cycle oscillations quickly diminish, and the airfoil settles into a static equilibrium. In this case, however, the system is stabilized with the flap positioned at one edge of the free-play region. Ideally, the system would reach an equilibrium with the flap in the center of the free-play zone. However, in practice imperfections in the airfoil result in small asymmetries in the aerodynamic forces on the airfoil. These asymmetries cause the system to come to rest off center.

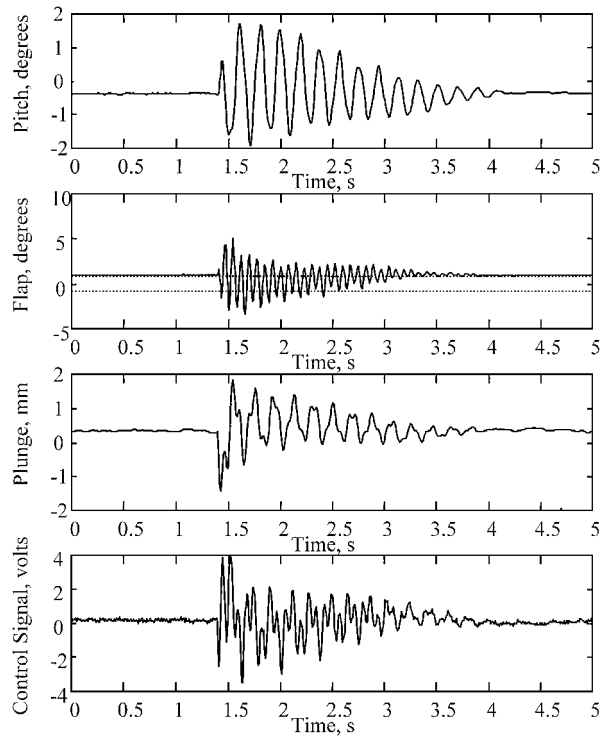

Fig. 9 Compensator performance beyond the open-loop flutter boundary, U = 19 m/s.

Flutter Control and Robustness

Although it has been demonstrated that the control approach is effective at eliminating LCOs, the control design can also increase the flutter velocity of the system. This is demonstrated in Fig. 9, which shows the system impulse response for $U = 19$ m/s and with the compensator designed for $U = 18$ m/s activated. Equal amplitude force impulses were applied to the plunge carriage mechanism with a modal hammer fitted with a force transducer. Note that the system in Fig. 9 is operating above the open-loop system flutter boundary. As is demonstrated in Fig. 9, the system is asymptotically stable under these conditions. This stability was maintained up to $U = 22$ m/s and remains stable. When the wing was excited at $U = 22$ m/s, then it entered a limit-cycle oscillation. Increasing the flow velocity any higher resulted in an unstable system. This represents a 17% increase over the open-loop flutter velocity.

Finally, the compensator design is also robust to significant variations in the flow velocity. This was demonstrated by closing the loop on the system and changing the flow speed in the wind tunnel. As an example, the $U = 18$ m/s compensator design was used to control the airfoil as the flow velocity was varied from $U = 0$ m/s up to $U = 22$ m/s. The system was stable throughout this range of flow speeds. An example of the system response is shown in Fig. 10,

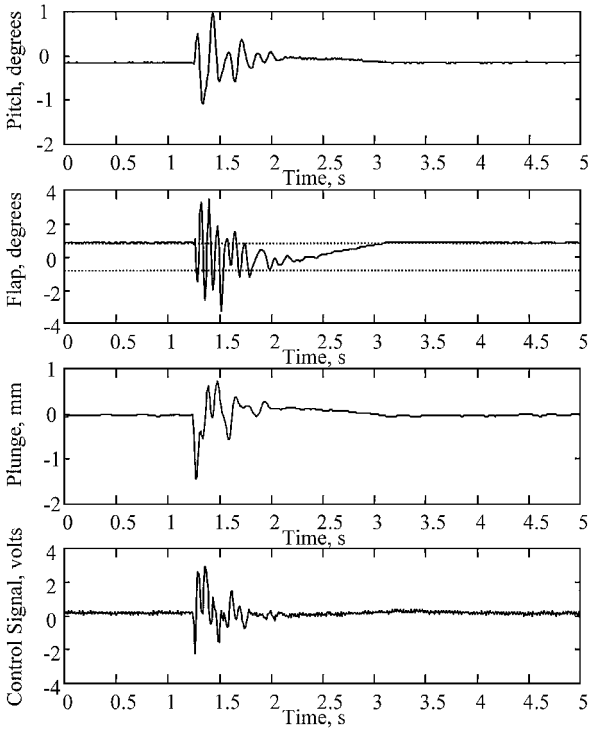

Fig. 10 Performance of the $U = 18$ m/s compensator at $U = 8$ m/s.

which shows the system impulse response at $U = 8$ m/s and with the control system designed at $U = 18$ m/s activated. Note that the compensator is very effective at eliminating LCO response. Similar behavior was noted throughout the flow-speed range of interest. This result could be of great benefit to control system designers. If a single compensator can be designed to control the system over a wide range of flight conditions, then a significant savings in system complexity and computation would be realized.

Conclusions

An experimental investigation into the active control of LCOs in a typical section with free play has been described. The discussion included a description of the experimental model, the instrumentation and testing facilities, as well as the control system design process. Results presented demonstrated that this approach is effective at eliminating LCO behavior for the studied model. The control design was demonstrated to be robust and stable over a wide range of flow speeds. Furthermore, the flutter boundary was increased by 17%.

Acknowledgments

The authors would like to acknowledge the support of the AFOSR Grant #F49620-96-1-0385, Brian Sanders, Program Manager, Structural Mechanics Division. Thanks also to Earl Dowell and Deman Tang for their contributions to this work.

References

[1]Conner, M. D., Tang, D. M., Dowell, E. H., and Virgin, L. N., "Nonlinear Behavior of a Typical Airfoil Section with Control Surface Freeplay: A Numerical and Experimental Study," *Journal of Fluids and Structures*, Vol. 11, 1997, pp. 89–109.

[2]Vipperman, J. S., Clark, R. L., Conner, M., and Dowell, E. H., "Investigation of the Experimental Active Control of a Typical Section Airfoil Using a Trailing Edge Flap," *Journal of Aircraft*, Vol. 35, No. 2, 1998, pp. 224–229.

[3]Vipperman, J. S., Barker, J. M., Clark, R. L., and Balas, G. J., "Comparison of μ and H2-Synthesized Controllers on a Experimental Typical Section," *Journal of Guidance, Control, and Dynamics*, Vol. 22, No. 2, 1999, pp. 278–285.

[4]Clark, R. L., and Frampton, K. D., "Control of a Three Degree-of-Freedom Airfoil with Limit Cycle Behavior," *Journal of Aircraft* (to be published).

[5]Woolston, D. S., Runyan, H. L., and Byrdsong, T. A., "Some Effects of System Nonlinearities in the Problem of Aircraft Flutter," NACA TN 3539, 1959.

[6]Breitbach, E., "Effects of Structural Non-Linearities on Aircraft Vibration and Flutter," AGARD TR 665, 1977.

[7]McIntosh, S. C., Jr., Reed, R. E., and Rodden, W. P., "Experimental and Theoretical Study of Nonlinear Flutter," *Journal of Aircraft*, Vol. 18, No. 12, 1981, pp. 1057–1063.

[8]Turner, C. D., "Wing/Control Surface Flutter Analysis Using Experimentally Corrected Aerodynamics," *Journal of Aircraft*, Vol. 19, No. 4, 1982, pp. 342–344.

[9]Yang, Z. C., and Zhao, L. C., "Analysis of Limit Cycle Flutter of an Airfoil in Incompressible Flow," *Journal of Sound and Vibration*, Vol. 123, 1988, pp. 1–13.

[10]Tang, D. M., and Dowell, E. H., "Flutter and Stall Response of a Helicopter Blade with Structural Nonlinearity," *Journal of Aircraft*, Vol. 29, No. 5, 1992, pp. 953–960.

[11]Kousen, K. A., and Bendiksen, O. O., "Limit Cycle Phenomena in Computational Transonic Aeroelasticity," *Journal of Aircraft*, Vol. 31, No. 6, 1994, pp. 1257–1263.

[12]Edwards, J. W., Ashley, H., and Breakwell, J. V., "Unsteady Aerodynamic Modeling for Arbitrary Motions," *AIAA Journal*, Vol. 17, No. 4, 1979, pp. 365–374.

[13]Price, S. J., Lee, B. H., and Alighanbari, H., "Postinstability Behavior of a Two-Dimensional Airfoil with Bilinear and Cubic Structural Nonlinearities," *Journal of Fluids and Structures*, Vol. 9, No. 6, 1994, 175–193.

[14]Smart ID System Identification Software, Ver. 1, Active Control eXperts, Inc., Cambridge, MA, 1994.